Desalination and Water Treatment
www.deswater.com

doi: 10.5004/dwt.2021.27714

237 (2021) 137–145
October

Investigation of the kinetic properties of Co-La-Ce-B catalyst for sodium borohydride solutions to generate hydrogen for polymer electrolyte membrane fuel cell

Arzu Ekinci[a], Ömer Şahin[b], Sabit Horoz[c,*]

[a]*Department of Occupational Health and Safety, Siirt School of Health, Siirt University, Siirt, Turkey, 56100, email: aekinci@siirt.edu.tr*
[b]*Department of Chemical Engineering, Faculty of Engineering, Siirt University, Siirt, Turkey, 56100, email: omersahin@siirt.edu.tr*
[c]*Department of Electrical and Electronics Engineering, Faculty of Engineering, Siirt University, Siirt, Turkey, 56100, email: sabithoroz@siirt.edu.tr*

Received 2 April 2021; Accepted 9 August 2021

ABSTRACT

We report the synthesis of Ce supported-Co-La-B (Co-La-Ce-B) catalyst and its catalytic activity. The synthesized Co-La-Ce-B catalyst for the first time is used to obtain the maximum hydrogen production rate from hydrolysis of sodium borohydride ($NaBH_4$). The synthesized Co-La-Ce-B catalyst indicates an effective performance in the hydrogen production from the hydrolysis of $NaBH_4$. It is found that synthesized Co-La-Ce-B catalyst has a hydrogen production rate of 9,764.00 mL/min g and 19.63 kJ mol^{-1}. Moreover, hydrogen produced from $NaBH_4$ hydrolysis in the presence of a Co-La-Ce-B catalyst was used in polymer electrolyte membrane (PEM) fuel cell application. The open-circuit voltage of the single PEM fuel cell was measured at 0.87 V, which is higher than that of typical fuel cells. The efficiency value according to the power is 54%, while the efficiency value according to the ideal voltage is 71%.

Keywords: Catalyst; Hydrogen; Sodium borohydride; Polymer electrolyte membrane

1. Introduction

In order to alleviate the growing demand for high power density portable electronic devices, great attention is paid to fuel cells as a power source to replace lithium-ion batteries [1]. A fundamental challenge for these portable electronic devices right now is generating and storing controlled amounts of hydrogen without using high-temperature reformers with large heat signatures [2–5]. High-pressure tanks, adsorbents, and hydrogen storage materials are frequently used to store hydrogen. Chemical hydrogen storage is chosen over the other ways because the purity of created hydrogen, the speed with which hydrogen is produced, and the portability of hydrogen storage materials are all superior. When sodium borohydride ($NaBH_4$) with a high hydrogen content is hydrolyzed, a high hydrogen conversion rate is produced. 1 g $NaBH_4$ can theoretically create 0.213 g hydrogen. Eq. (1) depicts the hydrolysis reaction [6–8].

$$NaBH_4 + 2H_2O \rightarrow NaBO_2 + 4H_2 \tag{1}$$

Noble metal catalysts and non-noble metal catalysts are both viable catalysts for the hydrolysis process of $NaBH_4$. Ruthenium (Ru) has been revealed to have a noticeable positive influence on the generation of hydrogen in the

---

* Corresponding author.

hydrolysis of $NaBH_4$ [9–12]. Pt@TiO_2 and Pt@CoO catalysts were created using the supercritical technique and showed good catalytic activity [13,14]. Non-noble metal catalysts, such as Co-B and Ni-B, are favored over noble metal catalysts because of their lower cost and better catalytic activity [13,15]. The chemical reduction was used to synthesize Ru, Co, Ni, Fe, Mn, and Cu catalysts. Ru has greater catalytic activity than Co and Ni, but Mn, Fe, and Cu have very low or non-existent catalytic activity [16–20]. Patel et al. [5] compared the catalytic activity of Co-based catalysts containing various transition metals as co-catalysts, including Ni, Fe, Cu, Cr, Mo, and W, and discovered that all of the Cr, W, Mo, and Cu can help Co-B catalyst increase its catalytic ability, whereas Ni and Fe have a relatively minor effect [21–25].

In the present report, the catalytic activity of the amorphous nanostructured Co-La-Ce-B catalyst synthesized by the chemical precipitation and reduction method was investigated. It was observed that the surface area of the Co-La-Ce-B catalyst increased due to the presence of lanthanum (La) and cerium (Ce) dopant metals, and therefore it showed higher catalytic activity. Factors affecting catalytic activity such as $NaBH_4$ and NaOH concentrations, reaction temperature and amount of catalyst were examined in the presence of Co-La-Ce-B catalyst and the maximum hydrogen production rate was determined for each factor. The activation energy was estimated by the Arrhenius equation by performing at different temperatures, and the best quaternary catalyst was tested in a single polymer electrolyte membrane (PEM) fuel cell application with Pt/C catalyst support for long-term use.

2. Materials and method

2.1. Materials

Cobalt(II) chloride hexahydrate ($CoCl_2·6H_2O$, 99.9%) was purchased from Alfa Aesar while cerium(III) nitrate hexahydrate ($Ce(NO_3)_3·6H_2O$, 99.9%), lanthanum(III) nitrate hexahydrate ($La(NO_3)_3·6H_2O$, 99.9%), sodium hydroxide (NaOH), sodium borohydride ($NaBH_4$, min 98%) and ethanol (C_2H_6O, technical grade) were purchased from Merck.

2.2. Synthesis of Co-La-Ce-B catalyst

In the study, the quaternary Co-La-Ce-B catalyst, which has not been applied before in hydrolysis of $NaBH_4$, was synthesized by the chemical precipitation and reduction method [26]. The full production of the catalyst is presented below.

1.30 g of $La(NO_3)_3·6H_2O$, 1.66 g of $CoCl_2·6H_2O$ and various concentrations (1%, 3%, 5%, 7%, and 10%) of $Ce(NO_3)_3·6H_2O$ were mixed in 800 mL of distilled water. The solution was left in an ice bath to maintain the temperature in the range of 0°C–5°C. Then, a certain amount of $NaBH_4$ was prepared in 50 mL of distilled water, and a black residue was obtained by adding dropwise to the metal mixture. It was washed several times with distilled water and ethanol to remove unwanted impurities from the solution. The synthesized Co-La-Ce-B catalyst was dried at 100°C in the presence of nitrogen gas. The obtained catalyst was stored in a closed box for use in hydrolysis experiments.

2.3. Hydrolysis of $NaBH_4$

$NaBH_4$ hydrolysis experiments were carried out under 10 mL solution volume, 25 mg catalyst amount and 2.5% $NaBH_4$ conditions. The volume of hydrogen obtained in $NaBH_4$ hydrolysis was determined by applying the cumulative method. The effects of metal ratio (for Ce), NaOH concentration, $NaBH_4$ concentration, catalyst amount and temperature parameters were investigated in $NaBH_4$ hydrolysis experiments. Moreover, the activation energy was estimated by the Arrhenius equation by performing at different temperatures.

2.4. PEM fuel cell application

Pt/C catalyst was used in the anode and cathode parts of the designed single-cell PEM fuel cell. Hydrogen produced from $NaBH_4$ hydrolysis in the presence of a Co-La-Ce-B catalyst was tested in the designed single-cell PEM fuel cell. Current-voltage-power generation values obtained from constant load were observed with measurements performed at regular time intervals.

2.5. Characterization

The X-ray diffraction (XRD) measurements were carried out on a Bruker D5005 powder diffractometer scanning from 15° to 85° (2θ) at a rate of $0.02°s^{-1}$ using a Cu Kα radiation (λ = 0.15418 nm) source. The applied voltage and current were 50 kV and 35 mA, respectively. Scanning electron microscopy (SEM) was performed using a JEOL JSM 5800LV SEM electron microscope linked to an energy-dispersive X-ray spectrometer (EDX) equipped with a Si–Li diode (PGT). The samples were deposited onto scotch carbon and metalized by sputtering. A gold film ensures a good conductivity for the observation.

3. Results and discussion

3.1. Characterization

Fig. 1 indicates a SEM image of the Co-La-Ce-B catalyst prepared in this study. A plate-like structure was observed. The particle size was several tens to hundreds of nanometers and the specific surface area was measured to be 71 $m^2 g^{-1}$. EDX analysis shown in Fig. 2 revealed that the prepared catalyst consisted of Co, La, Ce and B. Ce in the prepared catalyst could be combined with Co during the reduction reaction of $CoCl_2$ with $NaBH_4$ used as a reducing agent.

Fig. 3 demonstrates the XRD patterns of the Co-La-Ce-B catalysts heated at different temperatures. It can be seen that one relatively broad dispersing peak appears near 2θ ≈ 45° for the Co-La-Ce-B catalyst heated at 300°K, indicating an amorphous structure. When the heating temperature gradually increases from 300°K to 548°K, the diffraction peaks emerge around 2θ = 41.42°, 50.64° and 55.71° are very clear. According to the JCPDS database, the (1 1 1), (2 0 0), (2 2 0) diffractions of cubic Co [27] are located at 2θ = 42.216°, 51.522° and 55.853° respectively. The diffractions of metal La and Co are so closer, that they overlap with each other and cannot be distinctly identified in this case. At the same time, this phenomenon implies the

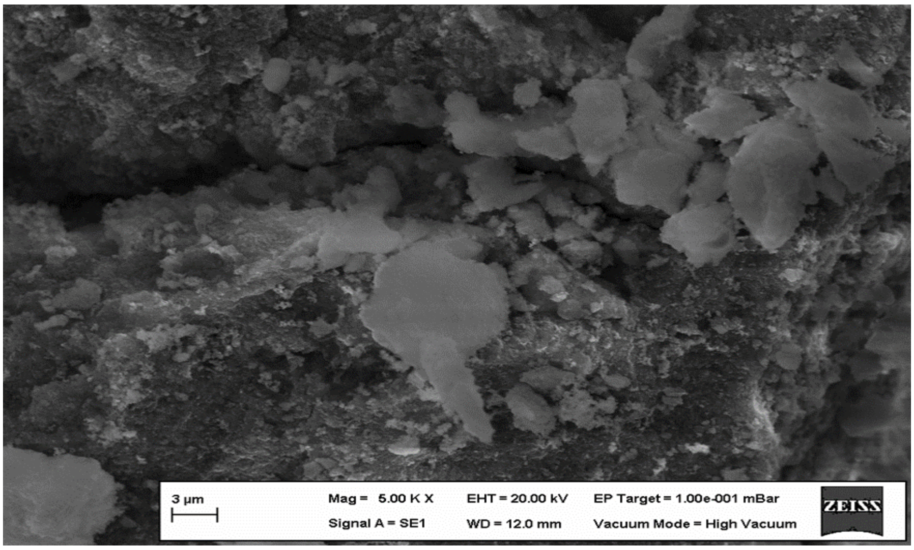

Fig. 1. SEM image of Co-La-Ce-B catalyst.

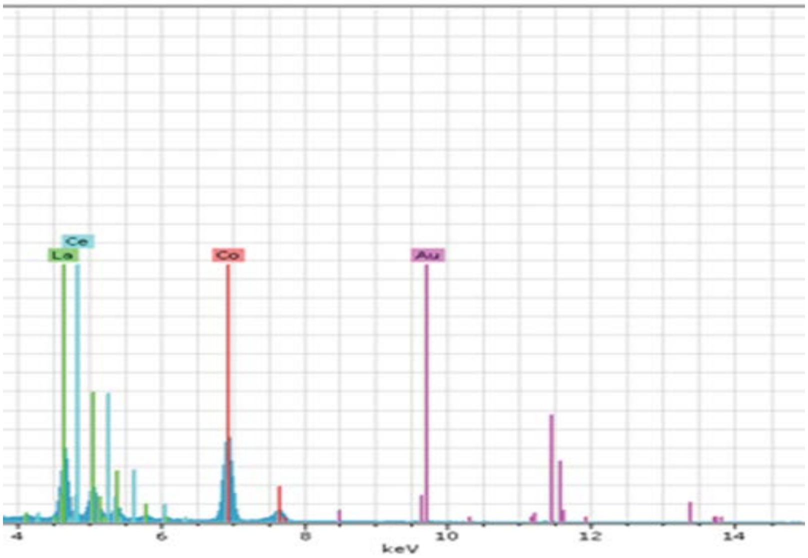

Fig. 2. EDX spectrum of Co-La-Ce-B catalyst.

formation of metal crystal states, especially a combination of metal La and Co, upon heat treating.

3.2. Catalytic activity of Co-La-Ce-B catalyst

3.2.1. Effect of Ce concentration

Fig. 4 reveals the graphs of hydrogen volume vs. time and hydrogen production rate vs. Ce concentration (%) in the presence of different Ce concentrations (1%, 3%, 5%, 7% and 10%). Experimental conditions were set at 30°C, 25 mg of Co-La-Ce-B catalyst, 2.5 wt.% NaOH and 2.5 wt.% $NaBH_4$.

It can be observed from Fig. 4 that the addition of Ce into the Co-La-Ce-B catalyst significantly promoted the hydrogen production rate. The hydrogen generation rate was appreciably enhanced by an increase of Ce concentration from 1%

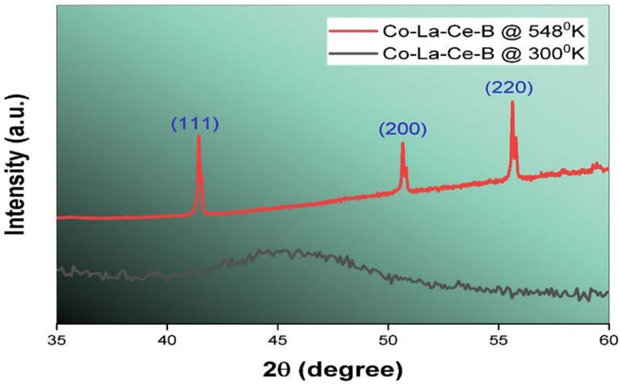

Fig. 3. XRD patterns of the Co-La-Ce-B catalysts heated at different temperatures: 300°K (black line) and 548°K (red line).

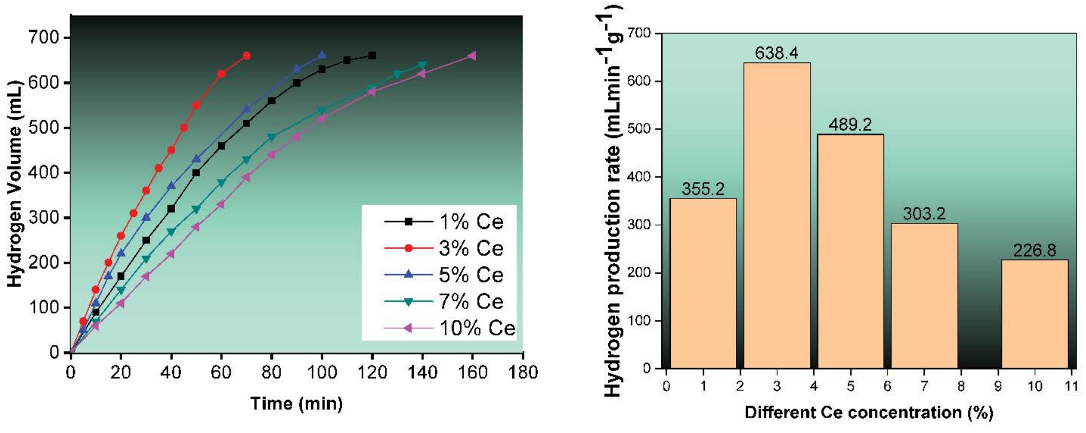

a

b

Fig. 4. Effect of Ce concentration on the hydrogen production in the presence of different Ce concentrations: (a) hydrogen volume vs. time and (b) hydrogen production rate vs. Ce concentration (%).

to 3%. However, when the ratio increased to 10%, the rate gradually decreased. The reason could be explained. On one hand, a slight Ce addition improved the dispersion of Co substance on the surface of the carriers. On the other hand, the excess of Ce addition may cause the growth of Co grains, which undermine the catalytic activity of Co-based active phases. As a result, the catalyst provided the best catalytic activity when the Ce concentration remained at 10%.

3.2.2. Effect of NaOH concentration

NaOH plays an important role in the hydrolysis of chemical hydrides, such as providing stabilization. Fig. 5 reveals the graphs of hydrogen volume vs. time and hydrogen production rate vs. NaOH concentration (%) in the presence of different NaOH concentrations (0%, 2.5%, 5%, and 7.5%). Experimental conditions were set at 30°C, 25 mg of Co-La-Ce-B catalyst and 2.5 wt% $NaBH_4$. The completion times of $NaBH_4$ hydrolysis in the presence of 0%, 2.5%, 5%, and 7.5% of NaOH concentration were determined as 70.09, 15.02, 30.11 and 39.98 min, respectively. In the presence of 0%, 2.5%, 5%, and 7.5% of NaOH of NaOH concentration, hydrogen production rates were 638.80; 3,880.00; 2,855.60 and 2,092.00 mL/min g, respectively. It should be noted that the increase in NaOH concentration causes a decrease in the hydrogen production rate. It is thought that hydroxyl ions caused by the increase in NaOH concentration form a bifunctional surface reaction during direct adsorption to the surface of the catalyst. Thus, excessive OH concentration adversely affects the hydrolysis reaction and hydrogen production rate [28].

3.2.3. Effect of $NaBH_4$ concentration

The graphs of hydrogen volume vs. time and hydrogen production rate vs. $NaBH_4$ concentration in the presence of different $NaBH_4$ concentrations (1%, 2.5%, 5%, and 7.5%) are exhibited in Fig. 6. Experimental conditions

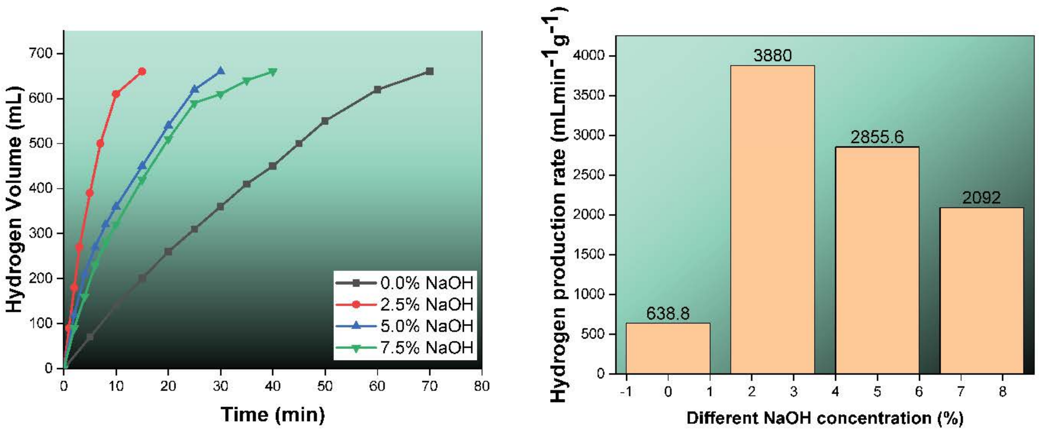

a

b

Fig. 5. Effect of NaOH concentration on the hydrogen production in the presence of different NaOH concentrations: (a) hydrogen volume vs. time and (b) hydrogen production rate vs. NaOH concentration (%).

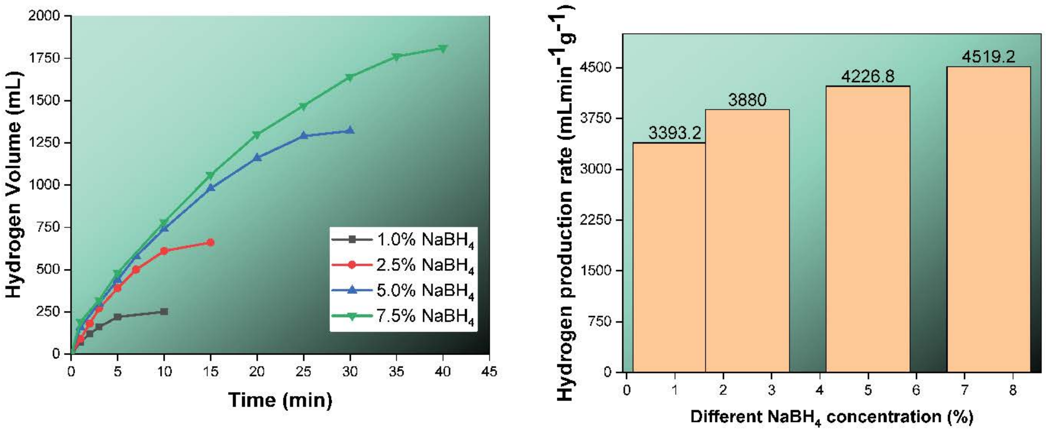

a

b

Fig. 6. Effect of $NaBH_4$ concentration on the hydrogen production in the presence of different $NaBH_4$ concentrations: (a) hydrogen volume vs. time and (b) hydrogen production rate vs. $NaBH_4$ concentration (%).

were set at 30°C, 2.5% NaOH and 25 mg of Co-La-Ce-B catalyst. The completion times of $NaBH_4$ hydrolysis in the presence of 1%, 2.5%, 5%, and 7.5% of $NaBH_4$ concentration were determined as 9.97, 15.02, 30.01 and 40.03 min, respectively. In the presence of 1%, 2.5%, 5%, and 7.5% of $NaBH_4$ concentration, hydrogen production rates were 3,393.20; 3,880.00; 4,226.80 and 4,519.20 mL/min g, respectively. As the concentration of $NaBH_4$ increases, the hydrolysis reaction of $NaBH_4$ is completed in a longer time but the hydrogen production rate increases. It must be noted that many researchers [6,29] had reported a low hydrogen production rate at both low and high $NaBH_4$ concentration, which was ascribed to the increase of solution viscosity. Clearly, the solution became more viscous with an increase in $NaBH_4$ concentration.

3.2.4. Effect of catalyst amount

The graphs of hydrogen volume vs. time and hydrogen production rate vs. catalyst amount in the presence of different amounts (10, 25, 50 and 70 mg) of Co-La-Ce-B catalysts are exhibited in Fig. 7. Experimental conditions were set at 30°C, 2.5% NaOH and 2.5 wt% $NaBH_4$. It is clear that the hydrolysis of $NaBH_4$ is significantly affected depending on the amount of catalyst. The completion times of $NaBH_4$ hydrolysis in the presence of 10, 25, 50 and 70 mg of Co-La-Ce-B catalyst were determined as 60.11, 15.02, 7.93 and 4.01 min, respectively. In the presence of 10, 25, 50 and 70 mg of Co-La-Ce-B catalysts, hydrogen production rates were 2,375.00; 3,880.00; 4,160.00 and 4,471.40 mL/min g, respectively. These results can be considered as an indication of how important the amount of catalyst is in the hydrogen production rate. When examining the effect of the catalyst amount on the hydrogen production rate, the point to be noted is the increase in the hydrogen production rate while the catalyst amount is increased from 10 mg to 70 mg. As expected, as the amount of catalyst increases, the reaction takes much less time to reach the estimated hydrogen production yield.

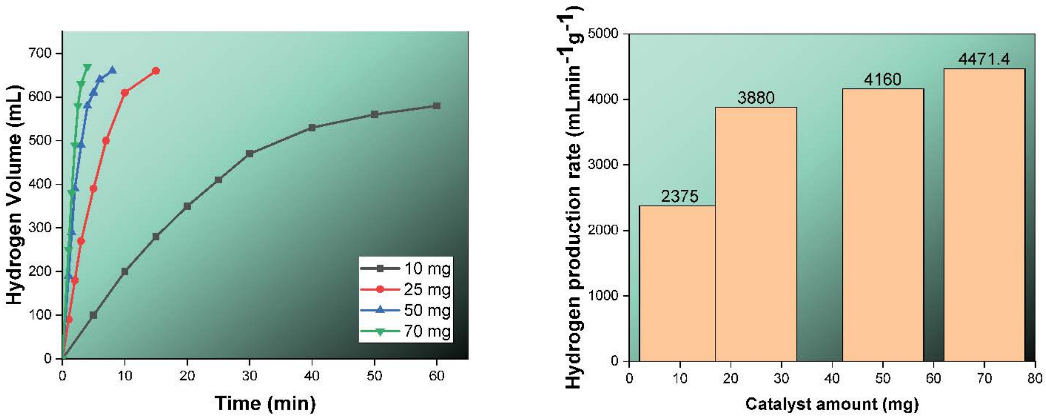

a

b

Fig. 7. Effect of catalyst amount on the hydrogen production in the presence of different Co-La-Ce-B catalyst amounts: (a) hydrogen volume vs. time and (b) hydrogen production rate vs. catalyst amount (mg).

3.2.5. Effect of temperature

Fig. 7 demonstrates the graphs of hydrogen volume vs. time and hydrogen production rate vs. temperature at different temperatures (30°C, 40°C, 50°C and 60°C). Experimental conditions were set at 25 mg of Co-La-Ce-B catalyst, 2.5% NaOH and 2.5 wt% $NaBH_4$. The completion times of $NaBH_4$ hydrolysis at 30°C, 40°C, 50°C and 60°C were determined as 15.02, 9.96, 7.98 and 4.94 min, respectively. At 30°C, 40°C, 50°C and 60°C, hydrogen production rates were 3,880.00; 5,173.18; 8,136.66 and 9,764.00 mL/min g, respectively. As can be clearly seen from Fig. 8, one of the most effective methods to complete the hydrolysis reaction in a shorter time and to have a higher hydrogen production rate is to increase the solution temperature. It is well known that an increase in solution temperature will accelerate the hydrogen production process.

In order to determine the activation energy (E_a), The Arrhenius plot given in Fig. 9 derived from the linear part of the plot for each temperature was used. The E_a of Co-La-Ce-B catalyst was derived as 19.63 kJ mol^{-1}, which is comparable to previously reported values for $NaBH_4$ hydrolysis. For comparison, the E_a values of the previously studied catalysts employed for the hydrolysis of $NaBH_4$ at room temperature are listed in Table 1. Obviously, the Co-La-Ce-B catalyst provides notable E_a value for the hydrolysis of $NaBH_4$ when compared with the other catalysts. The high catalytic activity of the Co-La-Ce-B catalyst may be attributed to the decrease in the mass transfer limitation in the liquid phase because of using Ce as doping material.

3.3. Performance of the single PEM fuel cell

Hydrogen produced from $NaBH_4$ hydrolysis in the presence of a Co-La-Ce-B catalyst was used in PEM fuel cell application. For the Co-La-Ce-B catalyst, the current-voltage-power curves showing the performance values of the PEM fuel cells are indicated in Fig. 10. The parameters used for the measurement were temperature: 50°C, solution volume: 10 mL, catalyst amount: 25 mg, resistance: 10 Ω. The open-circuit voltage of the single-cell PEM fuel cell was measured at 0.87 V, which is higher than that of typical fuel cells. The efficiency value according to the power is 54%, while the efficiency value according to the ideal voltage is 71%. The higher performance using the $NaBH_4$ hydrogen may be due to the fuel stream that carries saturated water vapor after the generator. In this case, the hydrogen gas does not additional humidification, which is clearly an advantage over dry hydrogen from a gas cylinder, which requires humidification before entering the fuel cell.

Table 1
The E_a values of some catalysts employed for the hydrolysis of $NaBH_4$ at the room temperature

Catalyst	E_a (kJ mol^{-1})	References
Co-La-B	42.33	[30]
Co-B/MWCNT	41.18	[31]
Co-Ce-B/Chi-C	33.10	[32]
Co-La-Ce-B	19.63	Current study
Ru/graphene	11.7	[33]

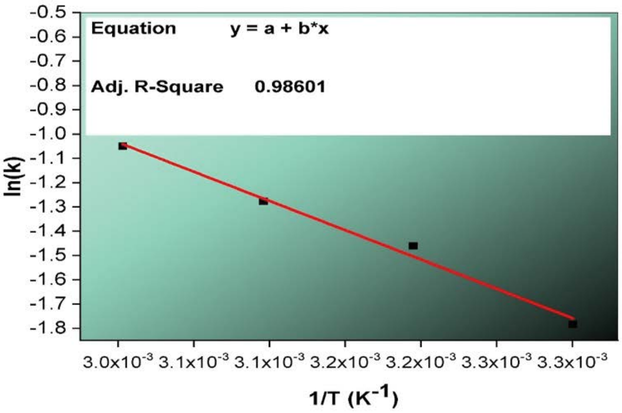

Fig. 9. The graph of ln*k* against 1/*T*.

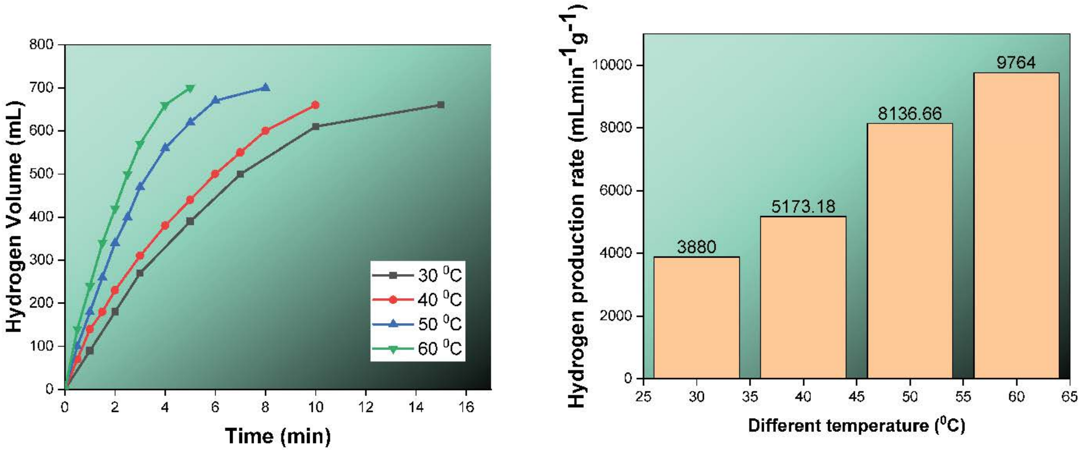

a

b

Fig. 8. Effect of temperature on the hydrogen production at different temperatures: (a) hydrogen volume vs. time and (b) hydrogen production rate vs. temperature (°C).

3.4. Kinetic study

According to Eq. (2), the borohydride anion (BH_4^-) and up to four water molecules are involved in the hydrolysis of aqueous alkaline $NaBH_4$ solution [34].

$$BH_4^-(aq) + 4H_2O \rightarrow B(OH)_4^-(aq) + 4H_2 \tag{2}$$

The rate of reaction (r) is proportional to the concentrations of BH_4^- and H_2O and may be expressed as a power law [34] is given in Eq. (3).

$$r \propto \left(BH_4^-\right)^{\alpha} \times \left(H_2O\right)^{\beta} \tag{3}$$

The second term, $(H_2O)^{\delta}$, might be regarded as constant when there is an excess of water. Following the evolution of the reaction rate as a function of the concentration of the hydroxide ions can also reveal the influence of solution alkalinity. The impact of the catalyst quantity can also be investigated. This is demonstrated by Eq. (4), which shows the reaction ordering (α, β, γ and δ) vs each of the aforementioned variables:

$$r \propto \left(BH_4^-\right)^{\alpha} \times \left(H_2O\right)^{\beta} \times \left(OH^-\right)^{\gamma} \times \left(\text{catalyst}\right)^{\delta} \tag{4}$$

The effect of increasing the catalyst amount on the r will not be explored in depth here because it is widely assumed that more active sites equal better kinetics. The reaction sequence of the catalyst amount should be in a positive order. Eq. (5) is obtained by taking the logarithm of both sides of Eq. (3).

$$\ln(r) = \ln(\text{hydrogen production rate}) \propto \alpha \times \ln\left(BH_4^-\right) \tag{5}$$

According to Eq. (5), the ln(hydrogen production rate) vs. ln($NaBH_4$) graph obtained in the presence of different $NaBH_4$ concentrations is shown in Fig. 11 (Catalyst amount (25 mg) and NaOH concentration (2.5%) were kept constant).

Based on Fig. 11, the r value was determined as 0.14 in the presence of different $NaBH_4$ concentrations. It was observed that the hydrogen production rate increased as the $NaBH_4$ concentration in the solution increased. The reaction rate and catalytic activity in zero-order kinetics are independent of BH_4^- concentration, implying that the quantity of BH_4^- adsorbed on the catalyst's surface is constant and the surface is saturated with adsorbed species [35].

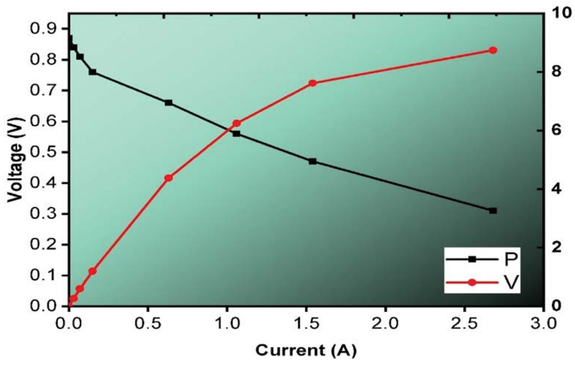

Fig. 10. Voltage–current and power–current curves.

It is possible to examine the OH^- effect in Eq. (6), which is obtained by keeping the BH_4^- and BH_4^- terms constant in Eq. (4) and taking the logarithm of both sides in Eq. (4).

$$\ln(r) = \ln(\text{hydrogen production rate}) \propto \gamma \times \ln\left(OH^-\right) \tag{6}$$

According to Eq. (6), the ln(hydrogen production rate) vs. ln(NaOH) graph obtained in the presence of different NaOH concentrations is shown in Fig. 12 (Catalyst amount (25 mg) and $NaBH_4$ concentration (2.5%) were kept constant). While the r value was determined as –0.55 in the presence of different NaOH concentrations, it was observed that the increase in the NaOH concentration negatively affected the hydrogen production rate. The probable cause of this situation can be attributed to the high OH^- anions preventing BH_4^- from being transferred to the catalyst surface [11].

Eq. (7) was used to determine the r value in the presence of different catalyst amount.

$$\ln(r) = \ln(\text{hydrogen production rate}) \propto \delta \times \ln(\text{catalyst}) \tag{7}$$

According to Eq. (7), the ln(hydrogen production rate) vs. ln(catalyst) graph obtained in the presence of different

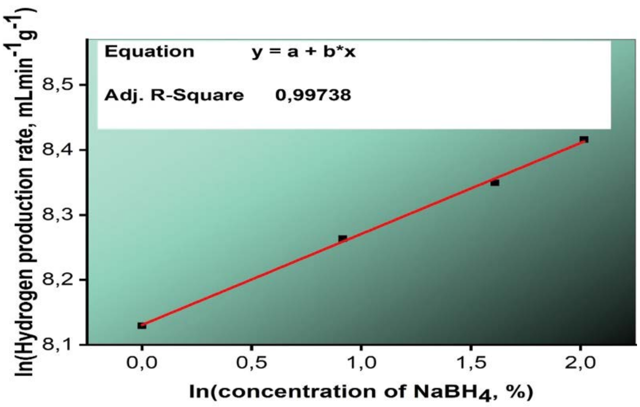

Fig. 11. The graph of ln(hydrogen production rate) vs. ln($NaBH_4$).

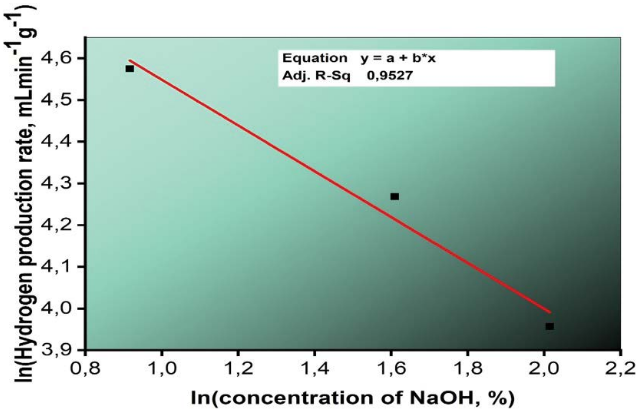

Fig. 12. The graph of ln(hydrogen production rate) vs. ln(NaOH).

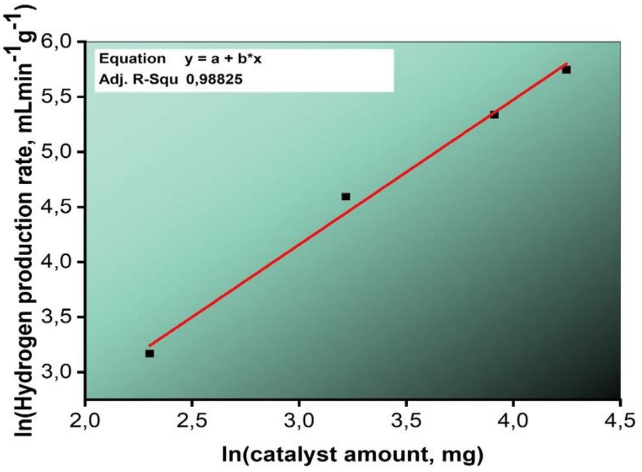

Fig. 13. The graph of ln(hydrogen production rate) vs. ln(catalyst).

NaOH concentrations is shown in Fig. 13 (NaOH concentration (2.5%) and $NaBH_4$ concentration (2.5%) were kept constant). While the *r* value was determined as 1.31 in the presence of different catalyst amounts, it was observed that the increase in the catalyst amount positively affected the hydrogen production rate. The possible reason for this situation is that the increase in the amount of catalyst provides the presence of more active surfaces [36].

The hydrolysis kinetics of NaOH stabilized $NaBH_4$ solutions were analyzed on the Co-La-Ce-B catalyst, and the hydrogen production rate is presented in Eq. (8).

$$r \propto \left(\mathrm{BH}_4^-\right)^{0.14} \times \left(\mathrm{OH}^-\right)^{-0.55} \times \left(\mathrm{catalyst}\right)^{1.31} \qquad (8)$$

This equation shows that hydrogen production rate depends on catalyst amount, $NaBH_4$ and NaOH concentration.

4. Conclusions

Ce supported Co-La-B (Co-La-Ce-B) was synthesized as a catalyst for hydrogen production from the hydrolysis of $NaBH_4$. Co-La-Ce-B catalyst was found to be active to produce hydrogen from aqueous $NaBH_4$. The maximum hydrogen production rate and activation energy of hydrogen production reaction in the presence of Co-La-Ce-B catalyst was 9764.00 mL/min g and 19.63 kJ mol^{-1}. It was observed that the Co-La-Ce-B catalyst gave high hydrogen efficiency and significantly reduced the reaction time of $NaBH_4$ hydrolysis. The high catalytic activity of the Co-La-Ce-B catalyst is associated with the mesoporous structure of catalyst. It can be concluded that high catalytic activity and simple synthetization process enable Co-La-Ce-B a very promising catalyst for on-board hydrogen production from the hydrolysis of $NaBH_4$. Moreover, hydrogen produced from $NaBH_4$ hydrolysis in the presence of Co-La-Ce-B catalyst was used in PEM fuel cell application. The open circuit voltage of the single PEM fuel cell was measured at 0.87 V, which is higher than that of typical fuel cells. The efficiency value according to the power is 54%, while the efficiency value according to the ideal voltage is 71%.

References

[1] S. Nar, Ö. Şahin, S. Horoz, Fabrication of pure Sb_2S_3 and Fe (2.5%): Sb_2S_3 thin films and investigation their properties, J. Inorg. Organomet. Polym. Mater., 29 (2019) 1331–1336.

[2] O. Baytar, M.S. Izgi, S. Horoz, O. Sahin, S. Nar, Al_2O_3 supported Co-Cu-B (Co-Cu-B/Al_2O_3) catalyst for hydrogen generation by hydrolysis of aqueous sodium borohydride ($NaBH_4$) solutions, Dig. J. Nanomater. Biostruct., 14 (2019) 673–681.

[3] R. Kothari, D. Buddhi, R. Sawhney, Comparison of environmental and economic aspects of various hydrogen production methods, Renewable Sustainable Energy Rev., 12 (2008) 553–563.

[4] L.V. Mattos, G. Jacobs, B.H. Davis, F.B. Noronha, Production of hydrogen from ethanol: review of reaction mechanism and catalyst deactivation, Chem. Rev., 112 (2012) 4094–4123.

[5] N. Patel, R. Fernandes, A. Miotello, Hydrogen generation by hydrolysis of $NaBH_4$ with efficient Co-P-B catalyst: a kinetic study, J. Power Sources, 188 (2009) 411–420.

[6] S.C. Amendola, S.L. Sharp-Goldman, M.S. Janjua, N.C. Spencer, M.T. Kelly, P.J. Petillo, M. Binder, A safe, portable, hydrogen gas generator using aqueous borohydride solution and Ru catalyst, Int. J. Hydrogen Energy, 25 (2000) 969–975.

[7] C. Lang, Y. Jia, J. Liu, H. Wang, L. Ouyang, M. Zhu, X. Yao, $NaBH_4$ regeneration from $NaBO_2$ by high-energy ball milling and its plausible mechanism, Int. J. Hydrogen Energy, 42 (2017) 13127–13135.

[8] X. Zhang, C. Li, J. Qu, Q. Guo, K. Huang, Cotton stalk activated carbon-supported Co-Ce-B nanoparticles as efficient catalysts for hydrogen generation through hydrolysis of sodium borohydride, Carbon Resour. Convers., 2 (2019) 225–232.

[9] O. Baytar, Investigation of high-activity activated carbon-supported Co-Cr-B catalyst in the generation of hydrogen from hydrolysis of sodium borohydride, Acta Chim. Slov., 65 (2018) 407–415.

[10] M.S. Izgi, C. Zörer, O. Baytar, Ö. Şahin, S. Horoz, Etkili Aktif Karbon Destekli CdS Fotokatalizörlerin Fotokatalitik Uygulamaları, Bitlis Eren Univ. J. Sci. Technol., 9 (2020) 662–670.

[11] R. Retnamma, A.Q. Novais, C. Rangel, Kinetics of hydrolysis of sodium borohydride for hydrogen production in fuel cell applications: a review, Int. J. Hydrogen Energy, 36 (2011) 9772–9790.

[12] Ö. Şahin, S. Kutluay, S. Horoz, M.Ş. Ece, Fabrication and characterization of 3,4-diaminobenzophenone-functionalized magnetic nanoadsorbent with enhanced VOC adsorption and desorption capacity, Environ. Sci. Pollut. Res., 28 (2021) 5231–5253.

[13] S.A. Al-Thabaiti, Z. Khan, M.A. Malik, Bimetallic Ag-Ni nanoparticles as an effective catalyst for hydrogen generation from hydrolysis of sodium borohydride, Int. J. Hydrogen Energy, 44 (2019) 16452–16466.

[14] W. Chen, L. Ouyang, J. Liu, X. Yao, H. Wang, Z. Liu, M. Zhu, Hydrolysis and regeneration of sodium borohydride ($NaBH_4$) – a combination of hydrogen production and storage, J. Power Sources, 359 (2017) 400–407.

[15] Y. Zou, M. Nie, Y. Huang, J. Wang, H. Liu, Kinetics of $NaBH_4$ hydrolysis on carbon-supported ruthenium catalysts, Int. J. Hydrogen Energy, 36 (2011) 12343–12351.

[16] I. Altuntas, M.N. Kocak, G. Yolcu, H.F. Budak, A.E. Kasapoğlu, S. Horoz, E. Gür, I. Demir, Influence of the PALE growth temperature on quality of MOVPE grown AlN/Si (111), Mater. Sci. Semicond. Process., 127 (2021) 105733, doi: 10.1016/j.mssp.2021.105733.

[17] M. Erdoğan, S. Horoz, Synthesis and characterization of a triphenylamine-dibenzosuberenone-based conjugated organic material and an investigation of its photovoltaic properties, J. Chem. Res., 45 (2021) 207–212.

[18] J. Guo, Y. Hou, B. Li, Y. Liu, Novel Ni-Co-B hollow nanospheres promote hydrogen generation from the hydrolysis of sodium borohydride, Int. J. Hydrogen Energy, 43 (2018) 15245–15254.

[19] K. He, G. Chen, G. Zeng, A. Chen, Z. Huang, J. Shi, M. Peng, T. Huang, L. Hu, Enhanced removal performance for methylene blue by kaolin with graphene oxide modification, J. Taiwan Inst. Chem. Eng., 89 (2018) 77–85.

[20] M. Ma, L. Yang, L. Ouyang, H. Shao, M. Zhu, Promoting hydrogen generation from the hydrolysis of Mg-Graphite composites by plasma-assisted milling, Energy, 167 (2019) 1205–1211.

[21] I. Dincer, C. Acar, A review on clean energy solutions for better sustainability, Int. J. Energy Res., 39 (2015) 585–606.

[22] N. Patel, A. Miotello, Progress in Co-B related catalyst for hydrogen production by hydrolysis of boron-hydrides: a review and the perspectives to substitute noble metals, Int. J. Hydrogen Energy, 40 (2015) 1429–1464.

[23] H. Schlesinger, H.C. Brown, A. Finholt, J.R. Gilbreath, H.R. Hoekstra, E.K. Hyde, Sodium borohydride, its hydrolysis and its use as a reducing agent and in the generation of hydrogen, J. Am. Chem. Soc., 75 (1953) 215–219.

[24] C. Wu, F. Wu, Y. Bai, B. Yi, H. Zhang, Cobalt boride catalysts for hydrogen generation from alkaline $NaBH_4$ solution, Mater. Lett., 59 (2005) 1748–1751.

[25] D. Xu, H. Wang, Q. Guo, S. Ji, Catalytic behavior of carbon supported Ni-B, Co-B and Co-Ni-B in hydrogen generation by hydrolysis of KBH_4, Fuel Process. Technol., 92 (2011) 1606–1610.

[26] A. Ekinci, E. Cengiz, M. Kuncan, Ö. Şahin, Hydrolysis of sodium borohydride solutions both in the presence of Ni-B catalyst and in the case of microwave application, Int. J. Hydrogen Energy, 45 (2020) 34749–34760.

[27] J. Lee, K.Y. Kong, C.R. Jung, E. Cho, S.P. Yoon, J. Han, T.-G. Lee, S.W. Nam, A structured Co-B catalyst for hydrogen extraction from $NaBH_4$ solution, Catal. Today, 120 (2007) 305–310.

[28] M. Ni, D.Y. Leung, M.K. Leung, A review on reforming bio-ethanol for hydrogen production, Int. J. Hydrogen Energy, 32 (2007) 3238–3247.

[29] S. Jeong, R. Kim, E. Cho, H.-J. Kim, S.-W. Nam, I.-H. Oh, S.-A. Hong, S.H. Kim, A study on hydrogen generation from $NaBH_4$ solution using the high-performance Co-B catalyst, J. Power Sources, 144 (2005) 129–134.

[30] J. Chang, F.L. Du, Investigation into hydrogen production in hydrolysis of sodium borohydride in the presence of Co-La-B catalyst, Adv. Mater. Res., 724 (2013) 735–739.

[31] Y. Huang, Y. Wang, R. Zhao, P.K. Shen, Z. Wei, Accurately measuring the hydrogen generation rate for hydrolysis of sodium borohydride on multiwalled carbon nanotubes/Co-B catalysts, Int. J. Hydrogen Energy, 33 (2008) 7110–7115.

[32] Y. Zou, Y. Yin, Y. Gao, C. Xiang, H. Chu, S. Qiu, E. Yan, F. Xu, L. Sun, Chitosan-mediated Co-Ce-B nanoparticles for catalyzing the hydrolysis of sodium borohydride, Int. J. Hydrogen Energy, 43 (2018) 4912–4921.

[33] N. Cao, W. Luo, G. Cheng, One-step synthesis of graphene supported Ru nanoparticles as efficient catalysts for hydrolytic dehydrogenation of ammonia borane, Int. J. Hydrogen Energy, 38 (2013) 11964–11972.

[34] U.B. Demirci, P. Miele, Reaction mechanisms of the hydrolysis of sodium borohydride: a discussion focusing on cobalt-based catalysts, C.R. Chim., 17 (2014) 707–716.

[35] D. Xu, X. Zhang, X. Zhao, P. Dai, C. Wang, J. Gao, X. Liu, Stability and kinetic studies of MOF-derived carbon-confined ultrafine Co catalyst for sodium borohydride hydrolysis, Int. J. Energy Res., 43 (2019) 3702–3710.

[36] O. Ozdemir, Analysis of kinetic properties for the hydrolysis reaction of $NaBH_4$ and environmental effects in the hydrogen production of activated Co-Ti(II)-B alloy catalysts, J. Faculty Eng. Archit. Gazi Univ., 34 (2019) 1585–1594.